

A New Double-Moment Microphysics Parameterization for Application in Cloud and Climate Models. Part I: Description

H. MORRISON

Department of Aerospace Engineering, University of Colorado, Boulder, Colorado

J. A. CURRY

School of Earth and Atmospheric Science, Georgia Institute of Technology, Atlanta, Georgia

V. I. KHVOROSTYANOV

Central Aerological Observatory, Dolgoprudny, Moscow, Russia

(Manuscript received 18 December 2003, in final form 24 September 2004)

ABSTRACT

A new double-moment bulk microphysics scheme predicting the number concentrations and mixing ratios of four hydrometeor species (droplets, cloud ice, rain, snow) is described. New physically based parameterizations are developed for simulating homogeneous and heterogeneous ice nucleation, droplet activation, and the spectral index (width) of the droplet size spectra. Two versions of the scheme are described: one for application in high-resolution cloud models and the other for simulating grid-scale cloudiness in larger-scale models. The versions differ in their treatment of the supersaturation field and droplet nucleation. For the high-resolution approach, droplet nucleation is calculated from Kohler theory applied to a distribution of aerosol that activates at a given supersaturation. The resolved supersaturation field and condensation/deposition rates are predicted using a semianalytic approximation to the three-phase (vapor, ice, liquid) supersaturation equation. For the large-scale version of the scheme, it is assumed that the supersaturation field is not resolved and thus droplet activation is parameterized as a function of the vertical velocity and diabatic cooling rate. The vertical velocity includes a subgrid component that is parameterized in terms of the eddy diffusivity and mixing length. Droplet condensation is calculated using a quasi-steady, saturation adjustment approach. Evaporation/deposition onto the other water species is given by nonsteady vapor diffusion allowing excess vapor density relative to ice saturation.

1. Introduction

The ability to accurately model cloud processes is of primary importance in correctly simulating the state of the atmosphere. Clouds exert a large influence on the shortwave and longwave radiative transfer, act as conduits for the conversion of water vapor to precipitation, and are an essential component of heat transfer through the release of latent heat. With increased computational ability, cloud and climate models are now able to incorporate sophisticated microphysics parameterizations for simulating cloud formation and evolution. These microphysics parameterizations are generally divided into two categories: bin models that explicitly calculate the evolution of the particle size distribution (e.g., Feingold et al. 1994; Khvorostyanov

1995; Stevens et al. 1996; Harrington et al. 1999; Jiang et al. 2001) and bulk models that represent the hydrometeor size with a distribution function (e.g., Lin et al. 1983; Rutledge and Hobbs 1983; Dudhia 1989; Ferrier 1994; Walko et al. 1995; Fowler et al. 1996; Meyers et al. 1997; Reisner et al. 1998). In 3D models with a large number of grid cells, parameterizations need to be fairly simple due to the significant computational cost for runs of even modest length. Thus, a balance must be achieved between the inclusion of detailed microphysics and the associated cost increase. Bin schemes are often not practical due to their computational expense; bulk models therefore present a viable alternative for many applications. For example, cloud-resolving simulations using bulk microphysics were able to replicate most features predicted with bin microphysics, but with at least two orders of magnitude less model integration time (Jiang et al. 2000).

Bulk microphysics schemes were initially developed for mesoscale modeling (e.g., Lin et al. 1983; Rutledge

Corresponding author address: Hugh Morrison, Dept. of Aerospace Engineering, University of Colorado, Boulder, CO 80309.
E-mail: hugh@cloud.colorado.edu

and Hobbs 1983; Dudhia 1989) These schemes included separate prognostic equations for the mixing ratios of cloud liquid, ice, rain, and one or more solid precipitation species (e.g., snow, graupel, hail) and included detailed parameterization of precipitation and evaporation/condensation processes. Bulk microphysics schemes were subsequently implemented and tested in climate models (e.g., Ghan and Easter 1992; Fowler et al. 1996; Lohmann et al. 1999; Curry et al. 2000) and have been widely used in cloud-resolving and large-eddy models (e.g., McCumber et al. 1991; Kruger et al. 1995; Wu et al. 1998; Xu and Randall 1996; Jiang et al. 2000).

An improvement in the representation of the hydrometeor size spectra in bulk schemes has been the prediction of two moments of the size distribution, that is, number concentration and mixing ratio (e.g., Levkov et al. 1992; Ferrier 1994; Harrington et al. 1995; Meyers et al. 1997; Reisner et al. 1998; Girard and Curry 2001). Predicting two moments of the size distribution increases the degrees of freedom associated with the hydrometeor spectra, improving calculations of the microphysical processes and radiative transfer (Meyers et al. 1997). However, these schemes typically predict number concentrations of either the ice/precipitation species (e.g., Ferrier 1994; Meyers et al. 1997) or the cloud droplets (e.g., Ghan et al. 1997); few schemes predict the number concentration of each species included in the model. As discussed in Part II of this paper (Morrison et al. 2005, hereafter Part II), both droplet and ice concentrations and sizes greatly impact the cloud microphysics and structure, particularly for mixed-phase clouds. Furthermore, simulations of the anthropogenic aerosol forcing of clouds should include a realistic treatment of the number concentration of each phase. Most studies have focused on aerosol modification of the droplet population (e.g., Albrecht 1989; Coakley and Walsh 2002; Ghan et al. 2001; Penner and Rotstain 2001; Feingold et al. 2003), but aerosol-ice interactions may also have a significant influence on ice and mixed-phase clouds (DeMott et al. 1997; Lohmann et al. 2001; Lohmann 2002).

To address these concerns, we have developed a new bulk microphysics scheme predicting the mixing ratios and number concentrations of droplets, cloud ice, rain, and snow. Detailed, physically based treatments of ice nucleation and droplet activation are incorporated allowing for the simulation of cloud-aerosol interactions in liquid, ice, and mixed-phase clouds. Two versions of the scheme are presented: one for application in high-resolution cloud models capable of resolving the supersaturation field (referred to as the resolved version), and the other for larger-scale models that generally cannot resolve the supersaturation (nonresolved version). New parameterizations are described in detail, and a prognostic formulation for the resolved supersaturation field is derived and tested. In Part II, the nonresolved version of the scheme is implemented into

a single-column model to simulate stratiform clouds observed during the Surface Heat Budget of the Arctic Ocean (SHEBA) field experiment.

2. Description of the microphysics parameterization

The system of equations for the new microphysics scheme contains kinetic equations for the mixing ratio, q , and number concentration, N , of each hydrometeor species in the model: cloud droplets, cloud ice, snow, and rain (eight total equations). The hydrometeor sizes are represented by gamma functions that are similar to observed size distributions (e.g., Rogers and Yau 1989, hereafter RY89; Pruppacher and Klett 1997, hereafter PK97). The microphysical processes in the scheme (a complete list is given in Table 1) represent the source/sink terms for q and N in the kinetic equations. A box

TABLE 1. List of the microphysical processes; N and P indicate change in number concentration and mixing ratio, respectively.

Process	Description
NIN	Ice nucleation from freezing of aerosol
NCN	Droplet activation from aerosol
NIMU	Ice multiplication
NRAU	Autoconversion of droplets to form rain
NSAU	Autoconversion of ice to form snow
NRAC	Accretion of droplets by rain
NSAC	Accretion of droplets by snow
NSAR	Accretion of rain by snow
NSAI	Accretion of cloud ice by snow
NIFT	Heterogeneous freezing of droplets to form cloud ice
NSFT	Heterogeneous freezing of rain to form snow
NIFM	Heterogeneous freezing of droplets to form cloud ice
NSFM	Heterogeneous freezing of rain to form snow
NRM	Melting of snow to form rain
NCM	Melting of cloud ice to form droplets
NCC	Self-collection of droplets
NIC	Self-collection of cloud ice
NSC	Self-collection of snow
NRC	Self-collection of rain
NIE	Loss of N due to sublimation of cloud ice
NRE	Loss of N due to evaporation of rain
NSE	Loss of N due to sublimation of snow
PID	Deposition/sublimation of cloud ice
PCD	Condensation/evaporation of droplets
PRD	Condensation/evaporation of rain
PSD	Deposition/sublimation of snow
PRAU	Autoconversion of droplets to form rain
PSAU	Autoconversion of cloud ice to form snow
PRAC	Accretion of droplets by rain
PSAC	Accretion of droplets by snow
PSAR	Accretion of rain by snow
PSAI	Accretion of cloud ice by snow
PIFT	Heterogeneous freezing of droplets to form cloud ice
PSFT	Heterogeneous freezing of rain to form snow
PIFM	Homogeneous freezing of droplets to form cloud ice
PSFM	Homogeneous freezing of rain to form snow
PRM	Melting of snow to form rain
PCM	Melting of cloud ice to form droplets
PIN	Ice nucleation from freezing of aerosol
PCN	Droplet activation from aerosol
PIMU	Ice multiplication

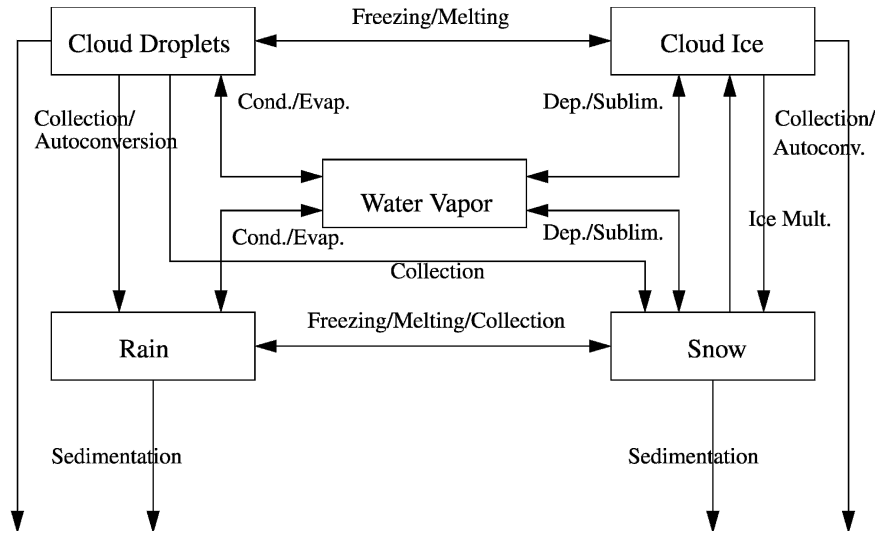


FIG. 1. Box diagram of the microphysics scheme.

diagram (Fig. 1) shows the relationship between the various water species and the microphysical processes that transit water between them. In the general 3D case, the kinetic equations for q and N depend on space variables x , y , and z and time, t ; that is, $q = q(x, y, z, t)$ and $N = N(x, y, z, t)$:

$$\begin{aligned} \frac{\partial q}{\partial t} = & -\nabla \cdot (\mathbf{v}q) + \frac{\partial}{\partial z} (V_{qx}) + \nabla_D q + \left(\frac{\partial q}{\partial t} \right)_{\text{PRO}} \\ & + \left(\frac{\partial q}{\partial t} \right)_{\text{COND/DEP}} + \left(\frac{\partial q}{\partial t} \right)_{\text{AUTO}} + \left(\frac{\partial q}{\partial t} \right)_{\text{COAG}} \\ & + \left(\frac{\partial q}{\partial t} \right)_{\text{MLT/FRZ}} + \left(\frac{\partial q}{\partial t} \right)_{\text{MULT}}, \end{aligned} \quad (1)$$

$$\begin{aligned} \frac{\partial N}{\partial t} = & -\nabla \cdot (\mathbf{v}N) + \frac{\partial}{\partial z} (V_{Nx}) + \nabla_D N + \left(\frac{\partial N}{\partial t} \right)_{\text{PRO}} \\ & + \left(\frac{\partial N}{\partial t} \right)_{\text{EVAP/SUB}} + \left(\frac{\partial N}{\partial t} \right)_{\text{AUTO}} + \left(\frac{\partial N}{\partial t} \right)_{\text{SELF}} \\ & + \left(\frac{\partial N}{\partial t} \right)_{\text{COAG}} + \left(\frac{\partial N}{\partial t} \right)_{\text{MLT/FRZ}} + \left(\frac{\partial N}{\partial t} \right)_{\text{MULT}}, \end{aligned} \quad (2)$$

where \mathbf{v} is the 3D wind vector, V_{Nx} and V_{qx} denote the number- and mass-weighted terminal particle fall speed for each species. Here we have included a turbulent diffusion operator ∇_D for models that parameterize turbulent mixing. The first three terms of the right-hand side of (1) and (2) involve spatial derivatives: advection, sedimentation, and turbulent diffusion. The remainder of the terms on the right-hand side of (1) and (2) are the microphysical processes. The last six terms in (1) are primary production (ice nucleation or droplet activation), condensation/deposition (evapora-

tion/sublimation), autoconversion (parameterized transfer of mass and number concentration from the cloud ice and droplet classes to snow and rain due to coalescence and diffusional growth), collection between hydrometeor species, melting/freezing, and ice multiplication (transfer of mass from the snow class to ice). The last seven terms in (2) are primary production, evaporation/sublimation, autoconversion, self-collection, collection between hydrometeor species, melting/freezing, and ice multiplication.

New parameterizations for prognostic supersaturation, droplet activation, heterogeneous and homogeneous ice nucleation, and the spectral index (width) of the droplet size distribution are developed in this paper and described in the remainder of the section. Formulations for hydrometeor collection (Beheng 1994; Passarelli 1978; PK97; Ikawa and Saito 1991; Murakami 1990), melting/freezing (Young 1974; Meyers et al. 1992; Rutledge and Hobbs 1984; Bigg 1953), autoconversion (Harrington et al. 1995; Beheng 1994), and ice multiplication (Hallet and Mossop 1974) are based upon existing parameterizations and described in the appendix.

a. Supersaturation

1) RESOLVED SUPERSATURATION

A realistic treatment of the supersaturation field is needed in high-resolution cloud models that calculate droplet activation using Kohler theory applied to a distribution of aerosol (e.g., Feingold et al. 1994; Stevens et al. 1996; Khvorostyanov et al. 2001; Jiang et al. 2001). In the general equation that includes all three water phases (i.e., vapor, liquid, ice), the evolution of supersaturation is controlled by vapor diffusion onto droplets and ice, and adiabatic (vertical air motion) and diabatic

(radiative) cooling. We derive an analytic approximation to the three-phase supersaturation equation that predicts the supersaturation field needed for the resolved droplet activation scheme described in section 2b(2). This solution may also be useful for bin models that calculate particle growth over a distribution of hydrometeors and thus require accurate treatment of the supersaturation. The direct numerical simulation used in some bin models to calculate supersaturation (e.g., Khvorostyanov 1995; Khvorostyanov et al. 2001) requires a time step less than the phase relaxation time-scale (<1–10 s for droplets) and is thus costly. The approach presented here does not have time step constraints for stability.

The three-phase supersaturation equation (e.g., Khvorostyanov 1995) is derived by differentiating the supersaturation ($\delta = q_v - q_{sw}$, where q_v is the water vapor mixing ratio and q_{sw} is the mixing ratio at water saturation) with time accounting for condensation/deposition onto the four hydrometeor classes included in the model: cloud droplets (c), cloud ice (i), rain (r), and snow (s):

$$\frac{d\delta}{dt} = -\left[\tau_c^{-1} + \tau_r^{-1} + \frac{Q_1}{Q_2}(\tau_i^{-1} + \tau_s^{-1})\right]\delta - \frac{Q_1}{Q_2} \times (\tau_i^{-1} + \tau_s^{-1})(q_{sw} - q_{si}) - \frac{dq_{sw}}{dT} \left[\left(\frac{\partial T}{\partial t}\right)_{\text{RAD}} - \frac{gw}{c_p} \right], \quad (3)$$

where T is the temperature, g is the gravitational acceleration, c_p is the specific heat of air at constant pressure, q_{si} is the ice saturation mixing ratio, $(\partial T/\partial t)_{\text{RAD}}$ is the radiative heating rate, τ is the phase relaxation time associated with each hydrometeor species (Khvorostyanov 1995; Khvorostyanov and Curry 1999b,c; Khvorostyanov et al. 2001), $Q_1 = 1 + (dq_{sw}/dT)(L_s/c_p)$, $Q_2 = 1 + (dq_{si}/dT)(L_s/c_p)$, and L_s is the latent heat of sublimation. The parameter τ has been modified here to include a size distribution integrated ventilation factor for falling particles (PK97):

$$\tau = \left\{ 2\pi\rho D_v C_0 N_0 \Gamma(p_c + 2) \left[\frac{f_1}{\lambda^{p_c+2}} + f_2 \left(\frac{ap}{\mu_a}\right)^{1/2} \text{Sc}^{1/3} \Gamma\left(\frac{b+2p_c+5}{2}\right) \lambda^{-(b+2p_c+5)/2} \right] \right\}^{-1}, \quad (4)$$

where f_1 and f_2 are ventilation coefficients given by PK97, a and b are fall speed parameters [see (A4) in appendix], D_v is the diffusivity of water vapor in air, ρ is the air density, μ_a is the dynamic viscosity of air, Sc is the Schmidt number, Γ is the Euler gamma function, and N_0 , p_c , and λ are the intercept parameter, spectral index, and slope of the hydrometeor size distribution, respectively [see (A1)–(A3) in appendix]. For cloud particles (i.e., droplets and cloud ice), ventilation effects are neglected. Here, the parameter C_0 relates the capacitance to the particle diameter or maximum di-

mension (i.e., capacitance = $C_0 D$). Capacitance arises from the analogy between the vapor diffusion equation and electrostatics involving a potential field, and describes the ability of a surface to store charge as a function of its size and shape (RY89; PK97). In the present version of the model, all hydrometeors are represented by spheres, giving $C_0 = 1$. Future versions of the scheme will take into account nonspherical ice particle habits.

The first term in (3) represents the loss (increase) in supersaturation due to condensation/deposition (evaporation/sublimation). The second term describes the flux of vapor from droplets to crystals, that is, the Bergeron–Findeisen mechanism. The third and fourth terms represent the generation (loss) of supersaturation due to radiative transfer and vertical air motion. An analytic solution to (3) requires additional assumptions due to the complex time dependence of τ , q_{sw} , q_{si} , dq_{sw}/dT , dq_{si}/dT . If they are constant during the model time step, then (3) gives a linear equation that yields the following expression:

$$\delta(t) = A\chi + (\delta_0 + A\chi) \exp\left(-\frac{t}{\chi}\right), \quad (5)$$

where

$$A = -\frac{Q_1}{Q_2}(\tau_i^{-1} + \tau_s^{-1})(q_{sw} - q_{si}) - \frac{dq_{sw}}{dT} \left[\left(\frac{\partial T}{\partial t}\right)_{\text{RAD}} - \frac{gw}{c_p} \right], \quad (6)$$

and χ is the general supersaturation relaxation time:

$$\chi = \left[\tau_c^{-1} + \tau_r^{-1} + \frac{Q_1}{Q_2}(\tau_i^{-1} + \tau_s^{-1}) \right]^{-1}. \quad (7)$$

Here δ_0 is the supersaturation at the beginning of the time step. The term A includes the Bergeron–Findeisen and Lagrangian supersaturation generation (loss) terms.

The condensation/deposition (evaporation/sublimation) rate averaged over the model time step (Δt) for cloud droplets (PCD) and cloud ice (PID) is given by

$$\text{PCD} = \frac{A\chi}{\tau_c} - \frac{\chi(\delta_0 - A\chi)}{\tau_c \Delta t} \exp\left[\left(\frac{\Delta t}{\chi}\right) - 1\right], \quad (8)$$

$$\text{PID} = \frac{A\chi + q_{sw} - q_{si}}{\tau_i} - \frac{\chi(\delta_0 - A\chi)}{\tau_i \Delta t} \times \exp\left[\left(\frac{\Delta t}{\chi}\right) - 1\right]. \quad (9)$$

Condensation/evaporation of rain (PRD) is given by (8) with τ_c replaced by τ_r . Deposition/sublimation of snow (PSD) is given by (9) with τ_i replaced by τ_s .

The condensation and deposition rates and supersaturation provided by the semianalytic approach do not vary by more than ~10% (with errors generally less than a few percent) from direct numerical simulation (second-order Runge–Kutta with a 0.01-s sub-time

step) using a time step between 5 and 300 s under a range of natural conditions, except in strongly nonequilibrium situations when the change in cloud water mixing ratio is large relative to the mixing ratio itself (error can exceed 50% if the time step is long, i.e., >3 min). However, strongly nonequilibrium conditions occur only briefly during formation and dissipation of the cloud, so that the overall error during the lifetime of the cloud is small. Furthermore, the time step should be small enough (less than tens of seconds) during cloud formation to resolve the maximum supersaturation as droplets activate [see section 2b(1)]. An advantage in using the semianalytic approach is that the solution is stable using a time step longer than the phase relaxation time scale; in the direct simulation, the time step must be less than the relaxation time scale for stability.

2) NONRESOLVED SUPERSATURATION

In large-scale model runs with a long time step, supersaturation is generally not resolved. Zero supersaturation is often assumed and the quasi-steady, saturation adjustment method (i.e., excess vapor is instantaneously converted to condensate) is used to calculate condensation rates. This approach is physically reasonable because the ratio of excess vapor (supersaturation) to droplet condensate is typically small due to short droplet phase relaxation time. However, phase relaxation associated with ice hydrometeors is typically much longer (>30 min). In a cooling air parcel, this can result in significant excess vapor density beyond ice saturation as is often observed (e.g., Heymsfield and Miloshevich 1995). Correspondingly, the amount of condensed ice relative to excess vapor may be quite small (e.g., Khvorostyanov et al. 2001; Khvorostyanov et al. 2005, hereafter K05). Therefore, the saturation adjustment approach is generally not appropriate for ice hydrometeors.

Taking into account these considerations, the nonresolved version of the scheme utilizes the saturation adjustment approach for cloud liquid water and the nonsteady, vapor diffusion approach for the other species (cloud ice, rain, snow) as is done in other bulk schemes (e.g., Ferrier 1994; Reisner et al. 1998). Droplet condensation is determined as follows (Dudhia 1989): Temperature, water vapor mixing ratio, and cloud water mixing ratio are forecast at the advanced time step (designated as T' , q'_v , q'_c) after all of the other physical processes have been calculated (including the microphysics). The supersaturation at the advanced time δ' is determined from q'_v and T' . The condensation rate is then given by

$$\text{PCD} = \frac{\delta'}{\Delta t} \left(1 + \frac{L_v^2 q'_{sw}}{c_p r_v T'^2} \right)^{-1}, \quad (10)$$

if $\delta' > 0$. If $\delta' < 0$, then evaporation of cloud water is given by

$$\text{PCD} = -\min \left[-\frac{\delta'}{\Delta t} \left(1 + \frac{L_v^2 q'_{sw}}{c_p r_v T'^2} \right)^{-1}, \frac{q'_c}{\Delta t} \right]. \quad (11)$$

Deposition/sublimation of cloud ice and snow is given by vapor diffusion (PK97):

$$\text{PID, PSD} = \frac{\delta_0}{Q_2 \tau} (q_{sw} - q_{si}), \quad (12)$$

where Q_2 and τ are defined in section 2a(1). This formulation allows excess vapor with respect to ice saturation. For evaporation of rain (PRD), the factor $(q_{sw} - q_{si})$ in (12) is removed, and Q_2 is replaced with $1 + (dq_{sw}/dT)(L_v/c_p)$. Note that condensation of rain is not allowed.

b. Droplet activation

According to Kohler theory, activation of droplets occurs on deliquesced soluble or partially soluble aerosols of a given size when a critical supersaturation is reached (e.g., RY89; PK97). In the model, dry aerosol is described by the Junge (1952) size distribution

$$f_a(r_D) = N_a (\mu - 1) r_{\min}^{\mu-1} r_D^{-\mu}, \quad (13)$$

where r_D is the dry aerosol radius, N_a is the total number concentration, r_{\min} is the radius of the smallest dry aerosol particle, and μ is the slope of the dry aerosol size distribution. The parameter r_{\min} provides a nonzero modal value for aerosol size spectrum, thereby preventing an unbounded number concentration at zero radius. The number of aerosol activated at a given supersaturation ratio $S = (q_v/q_{sw} - 1) \times 100\%$ is calculated following Khvorostyanov and Curry (1999a):

$$N' = \min(C_T S^k, N_a), \quad (14)$$

where

$$C_T = \frac{10^{-2k}}{k} 2N_a r_{\min}^{\mu-1} R \left(\frac{27b_a}{4B^3} \right)^R \quad (15)$$

and

$$k = \frac{\mu - 1}{1 + \beta}. \quad (16)$$

Values of b_a and β depend on the composition of the aerosol [see Khvorostyanov and Curry (1999a)], B is the Kelvin parameter, and

$$R = \frac{\mu - 1}{2(1 + \beta)}. \quad (17)$$

The activity spectrum of (14) has the form of the Twomey (1959) law. Equations (14)–(17) relate the Twomey expression to the aerosol number, size, and composition. The number nucleated is naturally bounded by the total aerosol concentration, which is important at high updraft velocity or low aerosol number (Abdul-Razzak et al. 1998). Observations (e.g., Hudson 1984) and numerical calculations (e.g., Feingold et al. 1994) have shown that k itself is a function of S . This variation of k may be interpreted in the context

of different mechanisms of aerosol formation leading to different slopes μ as a function of the aerosol radius (Khvorostyanov and Curry 1999a). Thus, a potential improvement in the representation of the aerosol size spectrum is to superimpose several spectra with differing values of C_T and k . We also acknowledge that this simple formulation does not account for chemical effects such as slightly soluble species and surfactants that can influence droplet activation (e.g., Nenes et al. 2002).

1) RESOLVED DROPLET ACTIVATION

In detailed cloud models with a time step on the order of tens of seconds or less and a grid spacing small enough to resolve processes that drive local cooling (e.g., vertical velocity), rapid changes in supersaturation are resolved and hence droplet activation may be explicitly calculated as a function of the aerosol properties and S following (14). This allows for a rigorous treatment of droplet nucleation needed for detailed simulation of cloud–aerosol interactions. To calculate the droplet activation rate, the maximum value of supersaturation ratio during the time step S_{\max} is determined from the resolved prognostic supersaturation [section 2a(1)]. The potential number of activated aerosol N' is calculated using S_{\max} for S in (14). The actual activation rate is determined by differencing the concentration of existing droplets (an estimate of the number of aerosols already activated) from N' similar to the methods of Stevens et al. (1996), Jiang et al. (2001), and others:

$$\text{NCN} = \max\left(\frac{N' - N_c}{\Delta t}, 0\right). \quad (18)$$

The change in cloud water mixing ratio due to droplet activation is given by $\text{QCN} = \text{NCN} \times m_{c0}$, where m_{c0} is the average mass of a newly activated droplet. It is assumed upon activation that droplets are described by the gamma size distribution.

Since prognostic aerosol is not considered in the present version of the scheme, changes in the aerosol size and chemical composition due to cloud–aerosol interactions are neglected. As pointed out by Feingold et al. (1999), these variations may have significant impact on the number of droplets activated under certain circumstances. Note also that kinetic effects on droplet growth were neglected in section 2a(1). Kinetic effects can influence the early growth of droplets and thus the activation rate depending on the condensation and thermal coefficients, and vapor and thermal jump lengths (Abdul-Razzak et al. 1998). For example, if the condensation coefficient is $\ll 1$, inclusion of kinetic effects may lead to slower droplet growth and thus larger values of S_{\max} and number concentration. We note that experimental values of the condensation and thermal coefficients are widely scattered between ~ 0.006 and 1 (PK97).

2) NONRESOLVED DROPLET ACTIVATION

In large-scale models with a time step longer than the time scale over which droplet activation occurs, that is, longer than tens of seconds (Abdul-Razzak and Ghan 2000), S_{\max} , and thus activation cannot be resolved. In this case, a parameterization for droplet activation must be based on numerical simulations of a cooling parcel. Furthermore, in large-scale models that are unable to resolve local cooling rates due to vertical motion, a parameterization for subgrid vertical velocity is needed since local cooling rates determine activation. Failure to account for subgrid vertical velocity may lead to serious underprediction of the number of droplets activated in large-scale models (Ghan et al. 1997; Part II).

A simple formulation is given below describing droplet activation with account for subgrid vertical velocity. For an activity spectrum of the form (14) consistent with the Twomey formulation, the potential number of droplets activated is given by (RY89)

$$N' = \min(0.88C_T^{2/(k+2)}(0.07w_{\text{ef}}^{3/2})^{k/(k+2)}, N_a), \quad (19)$$

where N' is in cm^{-3} and w_{ef} is the effective vertical velocity in cm s^{-1} . Here we employ an effective vertical velocity that takes into account diabatic heating due to radiative transfer (Khvorostyanov and Curry 1999b):

$$w_{\text{ef}} = w + w' - \frac{c_p}{g} \left(\frac{\partial T}{\partial t} \right)_{\text{RAD}}, \quad (20)$$

where w' is the characteristic subgrid-scale vertical velocity. Here, w corresponds with the large-scale (i.e., grid scale) value of vertical velocity.

The parameter N' represents the potential number of activated droplets; the actual number nucleated depends upon the existing number of cloud droplets:

$$\text{NCN} = \max\left(\frac{N' - N_c}{2\Delta t}, 0\right). \quad (21)$$

The factor of 2 accounts for the fact that both upward and downward subgrid vertical velocities are present in a grid cell, while activation only occurs in updrafts (Ghan et al. 1997).

This formulation implicitly assumes that aerosols are always available for nucleation at a given w_{ef} . Since the scheme assumes evaporation depletes number concentration only upon complete evaporation of the mixing ratio, negative subgrid vertical velocities do not cause a reduction in cloud number except indirectly through vertical mixing of droplets outside of the cloud. Therefore, only positive values of subgrid vertical velocity are assumed to influence droplet activation directly. The subgrid vertical velocity is parameterized in terms of a characteristic vertical velocity associated with turbulent mixing. We note that other processes can produce subgrid vertical motion (e.g., orography, gravity waves) but only consider turbulence here. As discussed by Ghan et al. (1997), the subgrid vertical velocity can either be

diagnosed from the turbulence kinetic energy if predicted or related to the vertical eddy diffusivity K .

A simple formulation for subgrid vertical velocity in terms of K is derived as follows: Assume a parcel is displaced from a reference level to z' with velocity w' (hereafter, prime denotes fluctuations, overbar is mean). If C is any scalar quantity, there is no mixing or other changes in C within a parcel, and the profile of C is linear, then the value of C at z' differs from its environment by C' , where

$$C' = -\left(\frac{\partial \bar{C}}{\partial z}\right) z'. \quad (22)$$

If the turbulence is characterized by a particular such that $|w'| \approx |\bar{w}'|$, $|C'| \approx |\bar{C}'|$, and $|z'| \approx m_l$, where m_l is the mixing length, then C' may be expressed in terms of K through first-order closure

$$\overline{w'C'} = -K\left(\frac{\partial \bar{C}}{\partial z}\right) \approx w'C'. \quad (23)$$

Combining (22) and (23) yields

$$w' \approx \frac{K}{m_l}. \quad (24)$$

This formulation for w' is similar to the standard deviation of vertical velocity derived by Ghan et al. (1997) (they have an additional factor of $\sqrt{2\pi}$ corresponding to a Gaussian distribution of vertical velocities). Here, however, w' is not strictly a function of the model vertical resolution but rather the mixing length. Nonetheless, it indirectly depends on the resolution; if the vertical resolution is coarse, gradients of potential temperature and wind shear will be poorly resolved leading to underprediction of w' . Thus, a lower bound for w' of 10 cm s^{-1} is specified as in Ghan et al. (1997). Simulations of droplet number concentration discussed in Part II exhibit only a small sensitivity to changes in the vertical resolution using this formulation.

Since this simple formulation uses a single value of w' to calculate droplet activation at each level in a grid cell, biases may occur since the subgrid vertical velocity in a grid cell is in reality characterized by some distribution and the relationship of N' to w' given by (19) is generally nonlinear. On the other hand, numerical integration of (19) using a distribution of w' is computationally costly and the actual distribution of w' in the atmosphere is uncertain. Further study is needed to better characterize the role of a distribution of w' in parameterizing droplet activation.

c. Homogeneous and heterogeneous ice nucleation

At temperatures warmer than approximately -35°C , ice particles form via heterogeneous nucleation on insoluble ice nuclei (IN). Because of its importance, heterogeneous nucleation has been studied extensively in the laboratory and field (e.g., Vali 1974; Deshler 1982;

Cooper 1986; Rogers 1982; Meyers et al. 1992; PK97). Empirical dependencies of IN concentration as a function of temperature or ice supersaturation have been suggested (e.g., Fletcher 1962; Cooper 1986; Meyers et al. 1992). Classical theory includes equations for the critical energy and radius of an ice germ to determine the nucleation rate per unit area of insoluble substrate. Khvorostyanov and Curry (2000, hereafter KC00) extended this theory to derive expressions for heterogeneous nucleation as a function of T and S with account for misfit strain. A major premise of this theory, similar to DeMott et al. (1997, 1999), is that internally mixed aerosol (i.e., particles containing both soluble and insoluble components) that serve as cloud condensation nuclei (CCN) may also serve as IN, but, as opposed to droplet activation, the insoluble fraction determines the activity of the nucleus. This formulation establishes a link between the temperature and humidity dependence and the aerosol physical and chemical characteristics.

Parcel simulations using the KC00 formulations were performed by Khvorostyanov and Curry (2005) and yielded reasonable values of N_i over a wide range of parameters. Significantly, the KC00 scheme produces realistic values of crystal concentration at cold temperatures ($<243 \text{ K}$) and can therefore be used to simulate heterogeneous ice formation in a wide range of cloud types. The commonly used Fletcher (1962) and Meyers et al. (1992) empirical parameterizations have often been arbitrarily modified at cold temperatures to avoid unrealistically large values of N_i (e.g., Reisner et al. 1998; Morrison et al. 2003).

In the model, heterogeneous nucleation on aerosol is assumed to occur by condensation freezing of deliquesced, internally mixed particles consisting of an insoluble nucleus surrounded by soluble material. The probability of condensation freezing of a particle with a radius of the insoluble portion of the aerosol, r_N , is expressed as

$$P_{\text{CF}} = 1 - \exp(-J_{\text{CF}}(r_N)\Delta t). \quad (25)$$

For the internally mixed particles described above, r_N is related to r_D by $r_N = r_D(1 - Q_v)^{1/3}$, where Q_v is the volume soluble fraction of the aerosol. The term J_{CF} is the rate of germ formation through condensation freezing (PK97):

$$J_{\text{CF}}(r_N) = \frac{kT}{h} \psi c_{1s} 4\pi r_N^2 \exp\left(-\frac{\Delta F_{\text{act}}}{kT} - \frac{\Delta F_{\text{cr}}}{kT}\right), \quad (26)$$

where k and h are Boltzmann's and Planck's constants, ψ is a preexponential factor incorporating the Zeldovich factor, the number of molecules in contact per unit area of ice germ, and the ice cap surface area, ΔF_{act} is the activation energy at the solution-ice interface, ΔF_{cr} is the critical energy of germ formation, and $c_{1s} = 10^{15} \text{ cm}^{-2}$ is the concentration of water molecules adsorbed on 1 cm^{-2} of a surface. The preexponential factor is

simplified by assuming $\psi \approx 1$ (PK97). Expressions for ΔF_{act} and ΔF_{cr} as a function of r_N , T , S , and the substrate parameters (e.g., misfit strain parameter, wettability coefficient, and relative area of active sites) are detailed in KC00.

At cold temperatures (less than -40°C), homogeneous freezing of submicron haze particles may be the dominant mode of ice formation (e.g., Sassen and Dodd 1989; Jensen et al. 1998). Khvorostyanov and Sassen (1998) express the critical energy and radius of an ice germ during homogeneous nucleation as a function of T and S . The nucleation rate expression is an extension of classical homogeneous nucleation theory for the three-phase (solution, ice, vapor) system. Homogeneous freezing occurs in either soluble or internally mixed particles. The probability of homogeneous freezing of a wet aerosol particle is expressed as

$$P_{\text{HF}} = 1 - \exp\left(-J_{\text{HF}}(r_w) \frac{4\pi}{3} (r_w^3 - r_N^3) \Delta t\right), \quad (27)$$

where the rate of germ formation per volume of solution, J_{HF} , is calculated following Khvorostyanov and Sassen (1998), and $r_w(r_D)$ is the radius of the hygroscopically grown aerosol with account for curvature and solute effects following Khvorostyanov and Curry (1999a).

The total probability of a particular particle freezing is

$$P_{\text{tot}} = P_{\text{CF}} + P_{\text{HF}} - P_{\text{CF}}P_{\text{HF}}, \quad (28)$$

based on the probability of freezing through either of the two mutually independent mechanisms operating simultaneously on the particle, limiting the total probability to unity. However, in most instances homogeneous and heterogeneous freezing would not be expected to act together since the humidity threshold for the onset of nucleation generally differs between the two mechanisms (K05).

The rate of ice nucleation associated with the polydispersed aerosol size distribution is given by

$$\text{NIN} = \frac{1}{\Delta t} \int_{r_{\text{min}}}^{r_{\text{max}}} f_a(r_D) P_{\text{tot}} dr_D, \quad (29)$$

where $f_a(r_D)$ is the dry aerosol size distribution given by (13), and r_{max} is the radius of the largest aerosol. The change in mixing ratio due to homogeneous and heterogeneous freezing of aerosol is given by $\text{PIN} = \text{NIN} \times m_{i0}$, where m_{i0} is the average mass of the nucleated crystal.

The loss of aerosol due to ice nucleation is not considered since S decreases rapidly after nucleation (by depositional growth onto the newly formed crystals), limiting the number of aerosol nucleation to a small fraction of the total aerosol (Khvorostyanov and Curry 2005). Note that this formulation assumes that changes in S associated with ice nucleation and crystal growth are resolved. A characteristic time scale for ice nucleation remains uncertain, although modeling evidence

suggests that it may be as short as a few seconds in some conditions (K05). These processes will not be temporally resolved in many applications potentially leading to an overprediction of the crystal concentration. Subgrid vertical velocity due to gravity waves (e.g., Jensen et al. 2005) or turbulence (K05) may also be important in nucleating ice in large-scale models. These issues will be considered in future parameterization development.

Owing to the complex time dependence of P_{tot} on r_D , (29) must be numerically integrated over the aerosol size distribution. To increase the computational efficiency, a 2D lookup table is used to determine NIN as a function of T and S for the assumed aerosol properties. The major drawback to this approach is that a new lookup table must be created if the aerosol parameters are modified; the dimensionality of the table would be far too large otherwise.

Nucleation directly from vapor (i.e., deposition nucleation) has not been included in the present formulation. In Part II, we assume that the aerosols have a sulfate coating that inhibits deposition nucleation, consistent with observations of the chemical composition of arctic aerosols (Borys 1989). This parameterization could be modified to account for deposition nucleation following KC00.

d. Droplet size distribution index

The index of the droplet size distribution determines the spectral dispersion, and is therefore important in calculating numerous microphysical processes that depend upon droplet size. For example, narrowing of the size spectra will tend to inhibit coalescence and freezing of the droplets (Khvorostyanov and Curry 1999c). Bulk microphysics parameterizations typically specify a constant value of p_c or spectral dispersion (e.g., Ferrier 1994; Girard and Curry 2001) or assume a monodisperse droplet population (e.g., Reisner et al. 1998). Observations (e.g., Curry 1986) show that the spectral dispersion varies substantially within the cloud. Khvorostyanov and Curry (1999b,c) derive a simple expression for the index of the droplet size distribution as a function of several cloud and thermodynamic parameters using an analytic solution to the general kinetic equation describing stochastic condensation:

$$p_c = \frac{w}{K} \frac{L_v A_c}{(g - \gamma_s c_p)}, \quad (30)$$

where w is the vertical velocity and K is the turbulent diffusion coefficient. The term w corresponds with the cooling rate and therefore should include subgrid vertical velocity, since values of p_c corresponding to the local size spectra determine the microphysical processes. If the local vertical velocity is characterized by turbulent mixing, then $w = K/m_l$ using first-order closure as discussed in section 2b(2) (m_l is the mixing length). Thus, an approximation to (30) is

$$p_c = \frac{1}{m_l} \frac{L_v q_c}{(g - \gamma_s c_p)}. \quad (31)$$

For a mixing length of 30 m following Williamson et al. (1987), values of p_c are calculated and compared with observations of arctic stratus (Curry 1986) in Table 2. Values of p_c calculated from (31) are somewhat smaller than observed; however, given uncertainty in values of m_l , the parameterization reasonably captures the vertical trend evident in the observations. The largest differences occur near cloud top. However, the observed spectra at cloud top are significantly influenced by entrainment and longwave radiative cooling (Curry 1986), which are neglected in the formulation of p_c . An expression similar to (31) for the cloud ice spectral dispersion will be developed for future versions of the scheme.

3. Summary and conclusions

A new four-class double-moment bulk microphysics scheme has been described. Prognostic equations include the mixing ratios and number concentrations of cloud droplets, cloud ice, rain, and snow. New, physically based parameterizations have been developed to simulate homogeneous and heterogeneous ice nucleation, droplet activation, and the dispersion of the droplet size distribution. Two versions of the scheme were described: one for large-scale models with lower spatial and temporal resolution and the other for higher-resolution applications. The two versions differ in their treatment of the supersaturation field and droplet activation.

For high-resolution models capable of resolving the maximum supersaturation, droplet activation is calculated from Kohler theory applied to a distribution of aerosol. This provides a detailed, physically based treatment of droplet activation for studying cloud–aerosol interactions (e.g., Feingold et al. 1994; Jiang et al. 2001). To account for the resolved supersaturation, a new parameterization was described based upon a semianalytic approximation to the three-phase (ice, vapor, liquid) supersaturation equation. This parameterization

does not have time step requirements for stability as in the direct numerical simulation.

For large-scale models typically run with a longer time step (~ 1 min or more), supersaturation cannot be resolved; thus, droplet activation is calculated using a simple parameterization that accounts for turbulence-generated subgrid vertical velocity. The quasi-steady saturation adjustment approach is used to predict droplet condensation that assumes zero residual supersaturation. However, evaporation/deposition onto the other water species (snow, rain, cloud ice) is calculated using nonsteady vapor diffusion. This formulation allows excess supersaturation with respect to ice.

The new scheme provides a detailed treatment of the microphysics for cloud and climate models at a reasonable computational cost (see Part II for detailed discussion of the cost). It can be utilized in process-oriented studies ranging in scales from global to regional to local depending upon the application. Since both versions of the scheme use grid-scale values of relative humidity to calculate the microphysics, the ability of the scheme to simulate various cloud types will depend upon the ability of the model to resolve the processes leading to cloud formation. This means that the scheme can predict grid-scale, generally stratiform clouds in large-scale models and convective or stratiform clouds in high-resolution models, assuming that convection can be explicitly resolved. Since the scheme incorporates close coupling between aerosol and cloud microphysics for liquid, ice, and mixed-phase clouds, it may be particularly useful for studying the influence of anthropogenic aerosol on clouds and radiation. After rigorous evaluation of the scheme's performance, it can be coupled to an aerosol microphysics model to provide a more detailed treatment of cloud–aerosol interactions and feedbacks. The new formulations presented here may also be applicable to bin-resolving microphysics schemes, namely, the treatments of ice nucleation, droplet activation, and prognostic supersaturation. The resolved version of the scheme is appropriate for large-eddy (LES) and cloud-resolving (CRM) models typically run at high spatial (< 1 km) and temporal (< 10 s) resolution. For large-scale climate models run with a longer time step, the nonresolved approach can be utilized. Modifications to the scheme could further improve its efficiency. For example, a variable time step could be incorporated so that the scheme uses a longer time step to calculate the microphysical processes except during droplet activation when a small time step is needed to resolve the maximum supersaturation.

Future work will improve the parameterization of several microphysical processes. Modeling of the ice phase remains particularly uncertain; for example, there are several assumptions inherent in the representation of the ice particle size spectrum, bulk density, and habit. Additional field measurements may help to reduce uncertainty in these parameters that vary widely depending upon local conditions (RY89; PK97). Bin-

TABLE 2. Observed (Curry 1986) and predicted values of the droplet spectral index, p_c , for observed cloud and thermodynamic conditions.

Date	Height (m)	q_c (g kg^{-1})	Observed p_c	Predicted p_c
20 Jun 1980	289 (top)	0.02	5.6	0.5
	241	0.34	10.1	8.7
	183	0.28	9.4	7.1
	91	0.16	6.7	4.1
28 Jun 1980	1082 (top)	0.03	5.9	0.5
	940	0.27	8.2	6.0
	819	0.09	5.3	2.0
	696 (base)	0.02	2.8	0.5

resolving simulations can also be used to better characterize the ice particle size distribution, which is important in predicting ice water content and number concentration (K05). Comparisons of the predicted microphysics using the new scheme with bin model results may be particularly useful for testing the scheme since ice microphysics parameters (e.g., mean particle size, crystal concentration) are often difficult to measure. The inclusion of graupel and/or hail microphysics (e.g., Rutledge and Hobbs 1984; Lin et al. 1983; Ferrier 1994; Meyers et al. 1997; Reisner et al. 1998) can improve the representation of ice-phase processes but also increases the complexity and cost. The addition of graupel microphysics to the scheme is described and tested in Part II. Another area of uncertainty is the impact of aerosol chemistry and composition on heterogeneous ice and droplet nucleation. For example, the presence of slightly soluble species, surfactants, and soluble gases can affect droplet activation (e.g., Charlson et al. 2001; Nenes et al. 2002). The relative area of active sites, wettability, and misfit strain parameter associated with the freezing mode on an insoluble substrate are generally not known a priori and can impact the ability of the aerosol to nucleate ice (PK97; KC00). Additional work will focus on improving these parameterizations by incorporating laboratory measurements and detailed numerical simulations (e.g., Nenes et al. 2001).

Acknowledgments. This research was supported by DOE ARM grant DE-FG03-94ER61771.

APPENDIX

Description of the Microphysical Processes

Each hydrometeor class is represented by a gamma size distribution of the form

$$f(D) = N_0 D^{p_c} e^{-\lambda D}, \quad (\text{A1})$$

where D is the diameter and p_c , N_0 , and λ are the spectral index, intercept, and slope, respectively. Values of p_c for droplets are a function of the cloud and thermodynamic properties (section 2d). At present, p_c is specified for cloud ice, rain, and snow. Expressions for λ and N_0 are given by

$$\lambda = \left[\frac{cN\Gamma(p_c + d + 1)}{q\Gamma(p_c + 1)} \right]^{1/d}, \quad (\text{A2})$$

$$N_0 = \frac{N\lambda^{p_c+1}}{\Gamma(p_c + 1)}, \quad (\text{A3})$$

where $m = cD^d$ is the assumed mass–diameter relationship. Occasionally, imbalances between the mass and number concentration can produce unrealistic values of λ . These imbalances may occur as a result of differential errors in advecting q and N ; these errors can be reduced by incorporating shape-preserving advection schemes (e.g., Smolarkiewicz 1983; Rasch and Williamson 1990).

Upper and lower bounds for λ are specified so that the mean particle diameter cannot exceed $30 \mu\text{m}$ or decrease below $0.1 \mu\text{m}$ for droplets, 250 and $0.1 \mu\text{m}$ for cloud ice, 1000 and $5 \mu\text{m}$ for rain, and 2000 and $5 \mu\text{m}$ for snow. The parameter λ is prevented from exceeding these bounds by appropriately adjusting the number concentration.

Terminal particle fall velocities are assumed to have the form

$$V_f(D) = (\rho_{\text{sur}}/\rho)aD^b, \quad (\text{A4})$$

where ρ_{sur} is the air density at sea level. Fall speeds for snow are given by the empirical relationships of Locatelli and Hobbs (1974) as a function of habit. For rain, $a = 841.99667 \text{ m}^{1-b}$ and $b = 0.8$ following Liu and Orville (1969). For cloud droplets and cloud ice, $a = 3 \times 10^7 \text{ m}^{1-b}$ and $b = 2$ and $a = 700 \text{ m}^{1-b}$ and $b = 1$, respectively (Ikawa and Saito 1991). Future versions of the scheme will incorporate expressions for the terminal fall velocities using power laws with continuous parameters over the size distributions following Khvorostyanov and Curry (2002) and Mitchell and Heymsfield (2005).

The increase in N_i due to rime splintering is a function of the liquid mass (rain and droplets) collected by snow (Hallet and Mossop 1974). Rime splintering is allowed in the temperature range $265.16 < T < 270.16$ K. The splintering of rime to form ice crystals also results in a transfer of mass from the snow class to the cloud ice class calculated by assuming splintered crystals have a diameter of $10 \mu\text{m}$.

Autoconversion represents the transfer of N and q from the droplet class to rain and cloud ice to snow due to growth by vapor diffusion and coalescence. The autoconversion of cloud droplets to rain is given by numerical simulations of droplet growth using stochastic collection (Beheng 1994). Since small crystals grow primarily by water vapor diffusion in many conditions (PK97), the autoconversion of cloud ice to snow is parameterized in terms of the vapor diffusion growth rate similar to Harrington et al. (1995):

$$\text{NSAU} = \left. \frac{dD}{dt} \right|_{D=D_b} f(D_b), \quad (\text{A5})$$

$$\text{PSAU} = \left. \frac{1}{\rho} \frac{dD}{dt} \right|_{D=D_b} f(D_b)m(D_b), \quad (\text{A6})$$

where dD/dt is the crystal growth rate (following from section 2a), f is size distribution, m is the particle mass, and $D_b = 125 \mu\text{m}$ (Harrington et al. 1995) is the threshold diameter delineating cloud ice from snow.

The self-collection (coalescence) of cloud droplets and rain is parameterized following Beheng (1994) based on numerical simulations of stochastic collection. The self-collection (aggregation) of cloud ice and snow follows from Murakami (1990) and Passarelli (1978), respectively. Collection between hydrometeor species

is parameterized by integrating the continuous collection equation (e.g., RY89; PK97) over the particle size distributions. Since experimental and theoretical evidence suggests that riming does not occur on ice particles smaller than $\sim 50\text{--}150\ \mu\text{m}$ depending on habit (PK97), collection of droplets by cloud ice is neglected. The accretion of cloud droplets by snow and rain is calculated using a simple gravitational collection kernel with fall speeds given by (A4); droplets are assumed to have a negligible fall speed in these calculations. Similarly, for collection of cloud ice by snow, fall speeds of ice are assumed to be negligible. The accretion of rain by snow is calculated following Ikawa and Saito (1991). Collisions between rain and cloud ice are neglected for simplicity. Rain and droplets are assumed to freeze instantaneously upon collision at temperatures below freezing. Collisions between liquid and ice species and between droplets and rain have a collection efficiency of 1, while collisions between ice species (including self-collection) have a collection efficiency of 0.1 following Reisner et al. (1998).

The heterogeneous freezing of cloud droplets and rain is assumed to occur through immersion and contact freezing (e.g., Lohmann et al. 2001). The formulation of immersion freezing follows from Bigg (1953). The formulation for contact freezing is based on a flux of contact IN to the drops due to Brownian motion, diffusiophoresis, and thermophoresis, with an effective diffusion coefficient given by Young (1974). The number of contact nuclei is given by Cooper (1986). Immersion freezing dominates at $T \lesssim -25^\circ$ to -15°C , while contact freezing is more important at warmer temperatures depending on drop size (freezing rates are a function of drop radius and volume for contact and immersion freezing, respectively). The freezing rates are integrated over the rain and droplet size distributions. Freezing of droplets and rain is allowed at $T < -4^\circ\text{C}$. The freezing of cloud droplets is a function of temperature and droplet size based on observations of mixed-phase stratus described by Rangno and Hobbs (2001). The droplet effective radius must be $\geq 12\ \mu\text{m}$ to initiate contact and immersion freezing of cloud droplets at $-10^\circ < T < -4^\circ\text{C}$. At $T < -10^\circ\text{C}$, contact freezing is allowed for all droplet sizes while droplet effective radius must be $\geq 10\ \mu\text{m}$ to initiate immersion freezing. Future versions of the scheme will incorporate more sophisticated formulations for heterogeneous droplet freezing allowing for cloud–aerosol interaction similar to the parameterization of condensation freezing of aerosol described in section 2c.

As a distribution of hydrometeors evaporates/sublimates, the smallest particles will completely dissociate into vapor. Failure to account for this loss may lead to unrealistically large number concentrations during evaporation or sublimation. Nonetheless, number concentration is assumed to be constant during evaporation of droplets following Ghan et al. (1997); simulations following Part II indicate that this assumption has

little impact since the droplet mixing ratio approaches zero quickly when conditions become subsaturated. For rain, snow, and cloud ice, the relative loss of number concentration is assumed to be equal to the relative loss of mixing ratio, so that λ remains constant during evaporation or sublimation.

Homogeneous freezing of cloud water and rain occurs instantaneously at temperatures below -40°C . Cloud ice is assumed to instantaneously melt at temperatures above 0°C . In water subsaturated conditions, melting cloud ice is assumed to evaporate instantaneously; in conditions of supersaturation, cloud ice melts to form droplets. Snow may persist above 0°C . The melting of snow to form rain and evaporation of melting snow in subsaturated conditions are calculated following Rutledge and Hobbs (1984).

REFERENCES

- Abdul-Razzak, H., and S. J. Ghan, 2000: A parameterization of aerosol activation, 2, Multiple aerosol types. *J. Geophys. Res.*, **105**, 6837–6844.
- , —, and C. Rivera-Carpio, 1998: A parameterization of aerosol activation, 1, Single aerosol type. *J. Geophys. Res.*, **103**, 6123–6131.
- Albrecht, B. A., 1989: Aerosols, cloud microphysics and fractional cloudiness. *Science*, **237**, 1020–1022.
- Beheng, K. D., 1994: A parameterization of warm cloud microphysical conversion processes. *Atmos. Res.*, **33**, 193–206.
- Bigg, E. K., 1953: The supercooling of water. *Proc. Phys. Soc. London*, **66B**, 688–694.
- Borys, R. D., 1989: Studies of ice nucleation by arctic aerosol on AGASP-II. *J. Atmos. Chem.*, **9**, 169–185.
- Charlson, R. J., J. H. Seinfeld, A. Nenes, M. Kulmala, A. Laaksonen, and M. C. Fachinini, 2001: Reshaping the theory of cloud formation. *Science*, **292**, 2025–2026.
- Coakley, J. A., Jr., and C. D. Walsh, 2002: Limits to the aerosol indirect radiative effect derived from observations of ship tracks. *J. Atmos. Sci.*, **59**, 668–680.
- Cooper, W. A., 1986: Ice initiation in natural clouds. *Precipitation Enhancement—A Scientific Challenge*, Meteor. Monogr., No. 43, Amer. Meteor. Soc., 29–32.
- Curry, J. A., 1986: Interactions among turbulence, radiation, and microphysics in Arctic stratus clouds. *J. Atmos. Sci.*, **43**, 90–106.
- , and Coauthors, 2000: FIRE Arctic Clouds Experiment. *Bull. Amer. Meteor. Soc.*, **81**, 5–29.
- DeMott, P. J., D. C. Rogers, and S. M. Kreidenweis, 1997: The susceptibility of ice formation in upper-tropospheric clouds to insoluble aerosol components. *J. Geophys. Res.*, **102**, 19 575–19 584.
- , Y. Chen, S. M. Kreidenweis, D. C. Rogers, and D. E. Sherman, 1999: Ice formation by black carbon particles. *Geophys. Res. Lett.*, **26**, 2429–2432.
- Deshler, T., 1982: Contact ice nucleation by submicron atmospheric aerosols. Ph.D. dissertation, University of Wyoming, 107 pp.
- Dudhia, J., 1989: Numerical study of convection observed during the Winter Monsoon Experiment using a mesoscale two-dimensional model. *J. Atmos. Sci.*, **46**, 3077–3107.
- Feingold, G., B. Stevens, W. R. Cotton, and R. L. Walko, 1994: An explicit cloud microphysical/LES model designed to simulate the Twomey effect. *Atmos. Res.*, **33**, 207–233.
- , W. R. Cotton, S. M. Kreidenweis, and J. T. Davis, 1999: Impact of giant cloud condensation nuclei on drizzle formation in marine stratocumulus: Implications for cloud radiative properties. *J. Atmos. Sci.*, **56**, 4100–4117.

- , W. L. Eberhard, D. E. Veron, and M. Previdi, 2003: First measurements of the Twomey indirect effect using ground-based remote sensors. *Geophys. Res. Lett.*, **30**, 1287, doi:10.1029/2002GL016633.
- Ferrier, B. S., 1994: A double-moment multiple-phase four-class bulk ice scheme. Part I: Description. *J. Atmos. Sci.*, **51**, 249–280.
- Fletcher, N. H., 1962: *The Physics of Rainclouds*. Cambridge University Press, 386 pp.
- Fowler, L. D., D. A. Randall, and S. A. Rutledge, 1996: Liquid and ice microphysics in the CSU General Circulation Model. Part 1: Model description and simulated microphysical processes. *J. Climate*, **9**, 489–529.
- Ghan, S. J., and R. C. Easter, 1992: Computationally efficient approximations to stratiform cloud microphysics parameterization. *Mon. Wea. Rev.*, **120**, 1572–1582.
- , L. R. Leung, and R. C. Easter, 1997: Prediction of cloud droplet number in a general circulation model. *J. Geophys. Res.*, **102**, 21 777–21 794.
- , and Coauthors, 2001: A physically-based estimate of radiative forcing by anthropogenic sulfate aerosol. *J. Geophys. Res.*, **106**, 5279–5293.
- Girard, E., and J. A. Curry, 2001: Simulation of Arctic low-level clouds observed during the FIRE Arctic Clouds Experiment using a new bulk microphysics scheme. *J. Geophys. Res.*, **106**, 15 139–15 154.
- Hallet, J., and S. C. Mossop, 1974: Production of secondary ice particles during the riming process. *Nature*, **249**, 26–28.
- Harrington, J. Y., M. P. Meyers, R. L. Walko, and W. R. Cotton, 1995: Parameterization of ice crystal conversion process due to vapor deposition for mesoscale models using double-moment basis functions. Part I: Basic formulation and parcel model results. *J. Atmos. Sci.*, **52**, 4344–4366.
- , T. Reisen, W. R. Cotton, and S. M. Kreidenweis, 1999: Cloud resolving simulations of Arctic stratus. Part II: Transition-season clouds. *Atmos. Res.*, **51**, 45–75.
- Heymsfield, A. J., and L. M. Miloshevich, 1995: Relative humidity and temperature influences on cirrus formation and evolution: Observations from wave clouds and FIRE II. *J. Atmos. Sci.*, **52**, 4302–4326.
- Hudson, J. G., 1984: Cloud condensation nuclei measurements within clouds. *J. Climate Appl. Meteor.*, **23**, 42–51.
- Ikawa, M., and K. Saito, 1991: Description of a nonhydrostatic model developed at the Forecast Research Department of the MRI. Meteorological Institute Tech. Rep. 28, 238 pp.
- Jensen, E. J., and Coauthors, 1998: Ice nucleation processes in upper-tropospheric wave clouds during SUCCESS. *Geophys. Res. Lett.*, **25**, 1363–1366.
- , and Coauthors, 2005: Formation of a tropopause cirrus layer observed over Florida during CRYSTAL-FACE. *J. Geophys. Res.*, **110**, D03208, doi:10.1029/2004JD004671.
- Jiang, H., W. R. Cotton, J. O. Pinto, J. A. Curry, and M. J. Weisbluth, 2000: Cloud resolving simulations of mixed-phase arctic stratus observed during BASE: Sensitivity to concentration of ice crystals and large-scale heat and moisture advection. *J. Atmos. Sci.*, **57**, 2105–2117.
- , G. Feingold, W. R. Cotton, and P. G. Duynkerke, 2001: Large-eddy simulation of entrainment of cloud condensation nuclei into the arctic boundary layer: May 18, 1998 FIRE/SHEBA case study. *J. Geophys. Res.*, **106**, 15 113–15 122.
- Junge, C. E., 1952: Die konstitution der atmosphärischen aerosols. *Ann. Meteor.*, **1**, 128–135.
- Khvorostyanov, V. I., 1995: Mesoscale processes of cloud formation, cloud-radiation and their modeling with explicit microphysics. *Atmos. Res.*, **39**, 1–67.
- , and K. Sassen, 1998: Cirrus cloud simulation using explicit microphysics and radiation. Part I: Model description. *J. Atmos. Sci.*, **55**, 1808–1821.
- , and J. A. Curry, 1999a: A simple analytical model of aerosol properties with account for hygroscopic growth, Part 1, Equilibrium size spectra and CCN activity spectra. *J. Geophys. Res.*, **104**, 2163–2174.
- , and —, 1999b: Towards the theory of stochastic condensation in clouds. Part I: A general kinetic equation. *J. Atmos. Sci.*, **56**, 3985–3996.
- , and —, 1999c: Towards the theory of stochastic condensation in clouds. Part II: Analytical solutions of the gamma distribution type. *J. Atmos. Sci.*, **56**, 3997–4013.
- , and —, 2000: A new theory of heterogeneous ice nucleation for application in cloud and climate models. *Geophys. Res. Lett.*, **27**, 4081–4084.
- , and —, 2002: Terminal velocities of droplets and crystals: Power laws with continuous parameters over the size spectrum. *J. Atmos. Sci.*, **59**, 1872–1884.
- , and —, 2005: The theory of ice nucleation by heterogeneous freezing of deliquescent mixed CCN. Part II: Parcel model simulation. *J. Atmos. Sci.*, **62**, 261–285.
- , —, J. O. Pinto, M. Shupe, B. A. Baker, and K. Sassen, 2001: Modeling with explicit spectral water and ice microphysics of a two-layer cloud system of altostratus and cirrus observed during the FIRE Arctic Clouds Experiment. *J. Geophys. Res.*, **106**, 15 099–15 112.
- , H. Morrison, J. A. Curry, D. Baumgardner, and P. Lawson, 2005: High ice supersaturation and modes of ice nucleation in thin tropopause cirrus: Simulation of the 13 July CRYSTAL case. *J. Geophys. Res.*, in press.
- Kruger, S. K., Q. Fu, K. N. Liou, and H.-N. S. Chin, 1995: Improvements of an ice-phase microphysics parameterization in numerical simulations of tropical convection. *J. Appl. Meteor.*, **34**, 281–287.
- Levkov, L., B. Rockel, H. Kapitzka, and E. Raschke, 1992: 3D mesoscale numerical studies of cirrus and stratus clouds by their time and space evolution. *Beitr. Phys. Atmos.*, **65**, 35–58.
- Lin, Y.-L., R. D. Farley, and H. D. Orville, 1983: Bulk parameterization of the snow field in a cloud model. *J. Climate Appl. Meteor.*, **22**, 1065–1092.
- Liu, J. Y., and H. D. Orville, 1969: Numerical modeling of precipitation and cloud shadow effects on mountain-induced cirrus. *J. Atmos. Sci.*, **26**, 1283–1298.
- Locatelli, J. D., and P. V. Hobbs, 1974: Fallspeeds and masses of solid precipitation particles. *J. Geophys. Res.*, **79**, 2185–2197.
- Lohmann, U., 2002: A glaciation indirect aerosol effect caused by soot aerosols. *Geophys. Res. Lett.*, **29**, 1052, doi:10.1029/2001GL014357.
- , N. McFarlane, L. Levkov, K. Abdella, and F. Albers, 1999: Comparing different cloud schemes of a single column model by using mesoscale forcing and nudging technique. *J. Climate*, **12**, 438–461.
- , J. Humble, W. R. Leaitch, G. A. Isaac, and I. Gultepe, 2001: Simulation of ice clouds during FIRE ACE using the CCCMA single-column model. *J. Geophys. Res.*, **106**, 15 123–15 138.
- McCumber, M., W. K. Tao, J. Simpson, R. Penc, and S. T. Soong, 1991: Comparison of ice-phase microphysical parameterization schemes using numerical simulations of convection. *J. Appl. Meteor.*, **30**, 985–1004.
- Meyers, M. P., P. J. DeMott, and W. R. Cotton, 1992: New primary ice nucleation parameterization in an explicit model. *J. Appl. Meteor.*, **31**, 708–721.
- , R. L. Walko, J. Y. Harrington, and W. R. Cotton, 1997: New RAMS cloud microphysics parameterization. Part II: The two-moment scheme. *Atmos. Res.*, **45**, 3–39.
- Mitchell, D. L., and A. J. Heymsfield, 2005: Refinements in the treatment of ice particle terminal velocities: Highlighting aggregates. *J. Atmos. Sci.*, **62**, 1637–1644.
- Morrison, H., M. D. Shupe, and J. A. Curry, 2003: Modeling clouds observed at SHEBA using a bulk microphysics parameterization implemented into a single-column model. *J. Geophys. Res.*, **108**, 4255, doi:10.1029/2002JD002229.

- , J. A. Curry, M. D. Shupe, and P. Zuidema, 2005: A new double-moment microphysics parameterization for application in cloud and climate models. Part II: Single-column modeling of arctic clouds. *J. Atmos. Sci.*, **62**, 1678–1693.
- Murakami, M., 1990: Numerical modeling of the dynamical and microphysical evolution of an isolated convective cloud—The July 19 1981 CCOPE cloud. *J. Meteor. Soc. Japan*, **68**, 107–128.
- Nenes, A., S. Ghan, H. Abdul-Razzak, P. Y. Chung, and J. H. Seinfeld, 2001: Kinetic limitations on cloud droplet formation and impact on cloud albedo. *Tellus*, **53**, 133–149.
- , R. J. Charlson, M. C. Fachinni, M. Kulmala, A. Laaksonen, and J. H. Seinfeld, 2002: Can chemical effects on cloud droplet number rival the first indirect effect? *Geophys. Res. Lett.*, **29**, 1848, doi:10.1029/2002GL015295.
- Passarelli, R. E., Jr., 1978: An approximate analytic model of the vapor deposition and aggregation growth of snowflakes. *J. Atmos. Sci.*, **35**, 118–124.
- Penner, J. E., and L. D. Rotstain, 2001: Indirect aerosol forcing, quasi forcing, and climate response. *J. Climate*, **14**, 2960–2975.
- Pruppacher, H. R., and J. D. Klett, 1997: *Microphysics of Clouds and Precipitation*. Kluwer Academic, 954 pp.
- Rangno, A. L., and P. V. Hobbs, 2001: Ice particles in stratiform clouds in the Arctic and possible mechanisms for the production of high ice particle concentrations. *J. Geophys. Res.*, **106**, 15 065–15 075.
- Rasch, A., and A. Williamson, 1990: Computational aspects of moisture transport in global models. *Quart. J. Roy. Meteor. Soc.*, **116**, 1071–1090.
- Reisner, J., R. M. Rasmussen, and R. T. Bruintjes, 1998: Explicit forecasting of supercooled liquid water in winter storms using the MM5 forecast model. *Quart. J. Roy. Meteor. Soc.*, **124**, 1071–1107.
- Rogers, D. C., 1982: Field and laboratory studies of ice nucleation in winter orographic clouds. Ph.D. dissertation, University of Wyoming, 161 pp.
- Rogers, R. R., and M. K. Yau, 1989: *A Short Course in Cloud Physics*. 3d ed. Pergamon Press, 293 pp.
- Rutledge, S. A., and P. V. Hobbs, 1983: The mesoscale and microscale structure and organization of clouds and precipitation in midlatitude cyclones. VIII: A model for the “seeder-feeder” process in warm-frontal rainbands. *J. Atmos. Sci.*, **40**, 1185–1206.
- , and —, 1984: The mesoscale and microscale structure and organization of clouds and precipitation in midlatitude cyclones. XII: A diagnostic modeling study of precipitation development in narrow cold-frontal rainbands. *J. Atmos. Sci.*, **41**, 2949–2972.
- Sassen, K., and G. C. Dodd, 1989: Haze particle nucleation simulation in cirrus clouds, and application for numerical and lidar studies. *J. Atmos. Sci.*, **46**, 3005–3014.
- Smolarkiewicz, P. K., 1983: A fully multidimensional positive definite transport algorithm with small implicit diffusion. *J. Comput. Phys.*, **54**, 325–362.
- Stevens, B., G. Feingold, W. R. Cotton, and R. L. Walko, 1996: Elements of the microphysical structure of numerically simulated nonprecipitating stratocumulus. *J. Atmos. Sci.*, **53**, 980–1006.
- Twomey, S., 1959: The nuclei of natural cloud formation, II, The supersaturation in natural clouds and the variation of cloud droplet concentration. *Geofis. Pura Appl.*, **43**, 243–249.
- Vali, G., 1974: Contact ice nucleation by natural and artificial aerosols. Preprints, *Conf. on Cloud Physics*, Tuscon, AZ, Amer. Meteor. Soc., 34–37.
- Walko, R., W. R. Cotton, M. P. Meyers, and J. Y. Harrington, 1995: New RAMS cloud microphysics parameterization. Part I: The single-moment scheme. *Atmos. Res.*, **38**, 29–62.
- Williamson, D. L., J. T. Kiehl, V. Ramanathan, R. E. Dickinson, and J. J. Hack, 1987: Description of the NCAR Community Climate Model (CCM1). NCAR Tech. Note NCAR/TN-285+STR, 112 pp.
- Wu, X., W. W. Grabowski, and M. W. Moncrieff, 1998: Long-term behavior of cloud systems in TOGA COARE and their interactions with radiative and surface properties. Part I: Two-dimensional modeling study. *J. Atmos. Sci.*, **55**, 2693–2714.
- Xu, K.-M., and D. A. Randall, 1996: Explicit simulation of cumulus ensembles with the GATE Phase III data: Comparison with observations. *J. Atmos. Sci.*, **53**, 3710–3736.
- Young, K. C., 1974: The role of contact nucleation in ice phase initiation in clouds. *J. Atmos. Sci.*, **31**, 768–780.

Copyright of Journal of the Atmospheric Sciences is the property of American Meteorological Society and its content may not be copied or emailed to multiple sites or posted to a listserv without the copyright holder's express written permission. However, users may print, download, or email articles for individual use.